Air Pollution Monitoring Model in Real-time with cloud based Channel Ranging and Stego Privacy Preservation

C. Radhakrishnan[1],* and Dr. R. Asokan[2]

[1]Assistant Professor, Department of Computer Science and Engineering, Kongunadu College ofEngineering and Technology, Thottiam, Trichy

[2]Professor, Department of Electronics and Communication Engineering, Kongunadu College of Engineering and Technology, Thottiam, Trichy

*Corresponding email: radhakrish.kongucse@gmail.com

Graphical Abstract

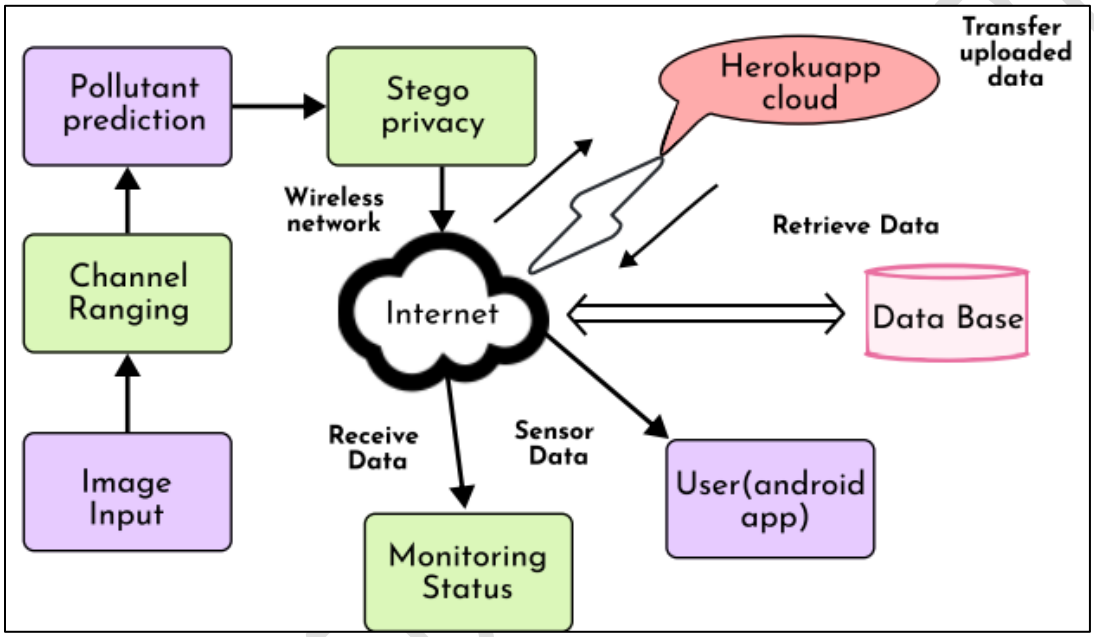

Abstract

In today's rapidly urbanizing world, the monitoring of air pollution has become imperative for safeguarding public health and the environment. Monitoring air quality in polluted environments is crucial for human health, but traditional methods using meteorological equipment have limitations in complex terrains and are costly. This study proposes a novel approach to address air pollution monitoring in urban areas by visually assessing the haziness of distant photos. This research explores the correlation between air quality indexes (e.g., AQI, PM2.5, PM10) and haziness levels in monitoring images. Results indicate that objective indicators accurately reflect air pollution levels, regardless of image size. To implement this observation practically, we introduce a new method called the "Channel ranging based prediction model in cloud with steganography-based privacy preservation framework." This model calculates a ratio between dark and bright channel information in scaled images, serving as a visual index of air pollution. By utilizing cloud infrastructure and sophisticated channel ranging mechanisms, the system intends to enhance the efficiency and reliability of air pollution monitoring, addressing both environmental concerns and privacy considerations in data transmission and storage. Experimental findings demonstrate the effectiveness of this metric in terms of correlation, computational speed, and classification accuracy compared to existing metrics. Particularly, the comparison of Pearson Correlation Coefficients (PCCs) across various image quality indices and

subjective ratings from the RHID_AQIs dataset reveals that the Channel ranging based cloud model achieves a PCC of 0.97, indicating strong correlation with image quality.

Keywords: Air quality monitoring, Cloud Model, Haziness, Privacy Preservation, Urban Pollution and Visual assessment

1 Introduction

The research is situated in the context of the pressing global issue of air pollution, which poses significant risks to public health and the environment. With rapid urbanization and industrialization, air quality monitoring has become increasingly important for identifying pollutants and mitigating their harmful effects. Traditional monitoring methods often face challenges in terms of accuracy, timeliness, and privacy protection of collected data. Therefore, there is a growing need for innovative approaches to address these limitations and enhance the effectiveness of air pollution monitoring systems.

Against this backdrop, the research aims to develop an advanced Air Pollution Monitoring Model capable of operating in real-time. By leveraging cloud-based channel ranging techniques and steganographic privacy preservation methods, the research seeks to overcome the shortcomings of existing monitoring systems. This includes improving the accuracy and immediacy of data processing while safeguarding the privacy of sensitive information.The background also emphasizes the importance of integrating cutting-edge technologies, such as cloud computing and steganography, into air pollution monitoring frameworks to enhance their efficiency and reliability. Furthermore, it underscores the significance of considering factors such as down-sampling parameters and window dimensions in optimizing the performance of the proposed model.Scholars have been investigating a range of vision-related remedies. For example, recommended utilizing video surveillance equipment to identify seasonal variations of the PM10 levels found in the surrounding atmosphere [Preethi *et al.* 2024], advised employing car detectors for recognizing cloud and airborne pollutants [Sallis *et al*. 2014], and offered an air degradation identification approach using instantaneous hyperspectral pictures [Mukundan et al. 2022].

In this study, we offer a new approach for detecting air pollution using surveillance photos that were motivated by the vision-oriented techniques mentioned above. The distinction is that our technique does not need any additional messages, includes detectors or hyperspectral information, it broadera variety of environmental classifications. There are two reasons behind the notion. Firstly, the continued advancement of imaging equipment has made it simple to observe images and videos via glasses, particularly in cities. In the domain of evaluating picture quality, several efficacious impartial markers are available [Wen *et al.* 2024] [Min *et al*.2019] [Li *et al*. 2019] [Wen *et al*. 2024] [Zhao *et al.* 2020] [Jiang *et al.* 2021] [Korthonen *et al*. 2019] [Du *et al.* 2013]. It goes without saying that visual quality cannot be compared to air quality. Nonetheless, prior investigations have demonstrated that particular metrics for assessing picture quality may accurately describe the degree of fog [Fu *et al.* 2013] [Kang *et al.* 2014] [Zhang *et al.* 2021] [Bosse *et a.* 2018] [Du *et al.* 2024] which is pertinent to the condition of the

atmosphere around you under foggy conditions. In their earlier study, we identified some indirect correlations among related external variables and the personal ratings in fuzzy pictures [Yin *et al.* 2023].

It is reasonable to inquire about the relationship between picture quality and air quality during hazy weather, given the current study results. Is it possible to use this kind of signal to describe the degree of air environmental damage? Yes, inasmuch as the object being snapped is literally revealed by the illumination origin, but the energy which it reflects is either absorbed or separated by air particles, creating an integral representation on the picture perception. Painting is like applying a filter to an item's reflections, provided that the item and source of light keep identical. diverse elements in the environment will impact the filter's effectiveness, producing diverse pictures.

In the meanwhile, the overall cleanliness of the atmosphere is correlated with its chemical make up. Therefore, by examining the variations in the photos, one may deduce the level of purity of the air. We conducted tests to investigate the association between objective assessment markers and pollution indices using our recently enhanced a dataset, RHID_AQI, in order to validate our previous findings. The collection consists of actual outdoor photos shot in eight different urban settings. The updated collection included the air polluted levels for every photo on the date that it was shot, in comparison to the previous version. The outcomes of the trial are positive. The degree of air pollution is shown to strongly correlate with picture quality. Thus, the current study proposes a quick assessment conduct utilizing surveillance images in large cities to represent the condition of the air. The primary action is to use a reduction approach and make use of the data found in the light and darkish channels of an unclear picture. The examination of the air condition is completed satisfactorily quickly, and the new approach is basic yet efficient. The novelty of the proposed work is,

- The research introduces a novel method for air pollution monitoring in urban areas by visually assessing haziness levels in distant photos. Departing from traditional meteorological equipment-based methods, this visual approach offers a cost-effective and versatile solution, particularly suited for complex terrains.
- The proposed "Channel ranging based prediction model in cloud with steganography-based privacy preservation framework" represents a pioneering advancement in air pollution monitoring. By calculating ratios between dark and bright channel information in scaled images, this model offers a unique visual index of air pollution. Its integration with cloud infrastructure and steganographic privacy preservation techniques enhances both efficiency and privacy in data transmission and storage.
- Through comprehensive experimentation, the research demonstrates the effectiveness of the proposed model in terms of correlation, computational speed, and classification accuracy. Particularly noteworthy is the high Pearson Correlation Coefficient (PCC) of 0.97 achieved by the Channel ranging based cloud model, indicating a robust correlation with image quality.

These key points underscore the novelty and practical applicability of the proposed approach in addressing air pollution monitoring challenges.

The remainder of the document is arranged as follows. Section 2 includes a detailed description of the suggested approach. We look into and contrast our metric's effectiveness to that of cutting-edge signals in the third section. Potential uses for real-time surveillance systems, such as those for air quality and other programs, are examined in Section 4, with findings presented in Section 5.

2 Datasets and Methodology

2.1 RHID_AQIs Datasets

Our research group created the RHID_AQI dataset for offering people with a blind standard for assessing the visual quality of fuzzy pictures [Du *et al*. 2024] [Yin *et al.* 2023]. The primary picture collection is from a 2014 Chinese photography exhibit [Ma *et al.* 2018], therefore we developed personal assessment studies on these photos using a single-stimulus approach. The archive was created using 301 photos that were captured in actual foggy settings within the metropolitan regions of eight contemporary Chinese cities.

In contrast to existing datasets on picture quality, the RHID_AQIs repository offers information regarding airborne pollutants. The AQIs coarse particulates (PM2.5) gauge, with inhalable particulates (PM10) indices are among ecological indices. Updated in the most recent edition is the classification and degree of air quality for every photograph.
As per the technical standards on the general [Shang *et al*. 2023], polluted air may be grouped into six distinct groups, and are displayed in Table 1. For categorization, we utilize the designations 0 and 1 to represent uncontaminated versus contaminated environments,

respectively.

Figure 1. Every environment's indicative picture from the RHID_AQIs dataset. These are the cities listed in order of importance

Table 1:AQIs with pollution level categories from the RHID_AQIs dataset.

AQIs	Level of AP	Various AP	Labels	Categories
0-50	L-1	Good	Zero	UN-Polluted
51-100	L-2	Moderate		
101-150	L-3	Polluted Lightly	One	Polluted
151-200	L-4	Polluted Moderately		
201-300	L-5	Polluted Heavily		
>300	L-6	Polluted Severely		

2.2 Subjective Indices Vs AQIs

First, let's go over the way subjective quality of images and the environment are related. Based on our earlier research, the cloudy image's subjective means opinions rating (MOS) approximately correlates adversely with the AQIs, PM2.5s, or PM10s airborne particle indicators, while the MOS numbers are in great agreement with the picture's appearance [Yin *et al.* 2023]. Using six images from the RHID_AQIs dataset that are spread over various ambient pollution rates in identical city, they illustrate this assertion by displaying the images' relative subjective ratings and AQIs ratings.

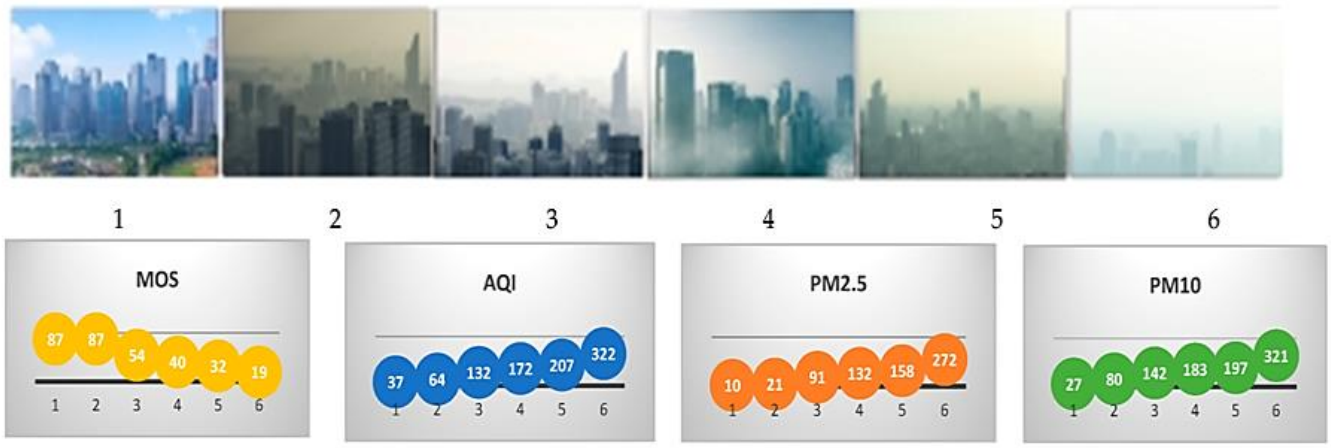

Figure 2. Variation tendency in ecological indices & subjective assessments for six photographs with varying pollutant rates. The a) MOS, b) AQIs, c) PM2.5, d) PM10 readings are listed in order of importance

It makes sense to notice that higher pollution levels and the absence of fog appear in images whenever atmospheric parameter standards, among them those for the AQIs, PM2.5s, PM10s, are lower. The pollutants in the air within the pictures progressively rises to a greater degree as environmental indicators rise. The conclusive multiple images even demonstrate misty & polluted air. There seems to be an adverse relationship among ecological indicators and personal

evaluations. We provide a scatter plot of the external versus internal MOS in Figure 3 along with an analysis of their Pearson correlation coefficients (PCC) to provide a more statistical illustration of this. The quantity of a linear connection among two signals, whose may be described as ensues, is often measured using the PCCs in Eq (1):

$$PCC = \frac{\sum_{i=1}^{M}(x_i - \bar{X})(y_i - \bar{Y})}{\sqrt{\sum_{i=1}^{M}(x_i - \bar{X})^2}\sqrt{\sum_{i=1}^{M}(y_i - \bar{Y})^2}} \quad (1)$$

M - overall amount of photos x_i&y_i indicate i^{th} picture quality & air pollution ratings, &X ,Y are the averages of the picture & airflow rankings in every picture set.

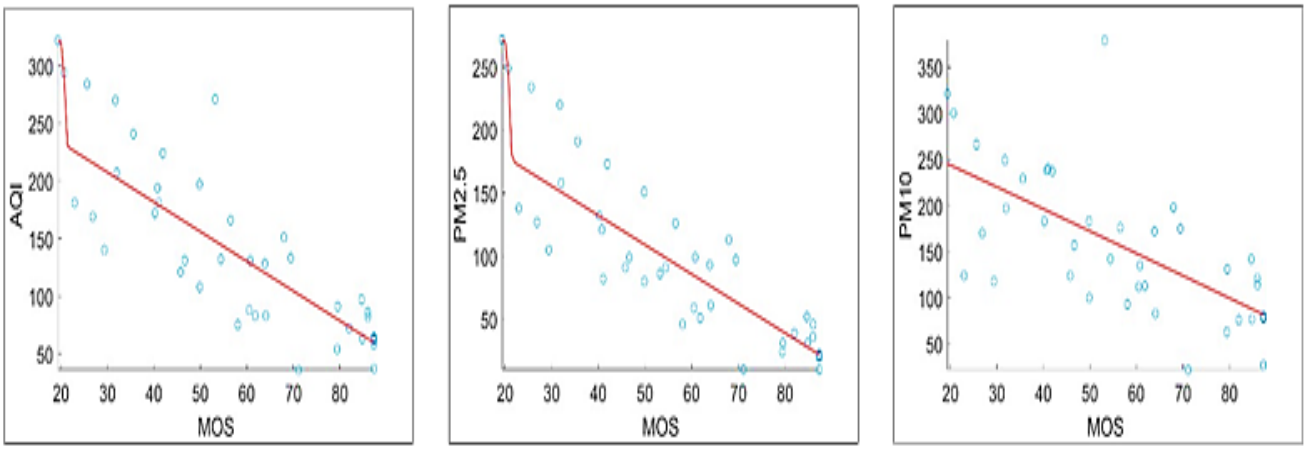

Figure 3. The RHID_AQIs collection contains scatter diagrams of MOSs readings against ambient indices for a Beijing area. PCCs = -0.86 for the AQIs, -0.90 for PM2.5s, and -0.68 for PM10s respectively

In addition, any potential for nonlinearity among anticipated image resolution ratings and air pollution data must be addressed before the assessment index is produced. As advised by the media image experts panel [Ancuti *et al.* 2020], a five-parameter quadratic logistic regression equation is used in this work Eq (2):

$$y = \beta_1 \left[\frac{1}{2} - \frac{1}{1 + e^{\beta_2(s-\beta_2)}}\right] + \beta_{4s} + \beta_5 \quad (2)$$

where y is the mapped target rating, s is the anticipated grade rating, and all model-fitting variables were β1 to β5. Figure 3 presents an impressive correlation of 89% for PM2.5 in addition to demonstrating a negative linear relationship among the air indicators of quality and the personal ratings. Since the amount of small particles, or PM2.5, is an important indicator of pollutants for weather experts [Kamani *et al.* 2023] [Oliveria *et al.* 2019] has greater public interest owing to its high significance to pulmonaries disorders, this strong correlate is advantageous for research on airborne pollutants.

3 Proposed Methodology

3.1 Motivation

Thus far, our findings indicate a strong correlation between subjective assessments of the hazy photographs and the parameters of the setting. This suggests that we may detect the air resolution by looking at the picture clarity to a certain degree. Subjective assessments of outside situations, however, are time-consuming, difficult, and unpleasant. For a view of the air excellence, experts recommend replacing the personal assessments in this portion with mechanically derived quantitative scores.

What kind of statistic is best for identifying air pollution, is the topic at hand. The most well-known and often used IQA measure is SSIM [Wang *et al.* 2004], which may be used for both versatile and full-reference image quality assessment. However, when we identify pollutants in foggy photographs, we don't have the initial hazy-free images to compare. SSIM is thus not applicable in this situation. Applicants for jobs involving an evaluation of levels of airborne pollutants must to be no-reference metric. Numerous outstanding techniques for evaluating the accuracy of no-reference photos exist. These methods may be used to the deterioration method for natural photographs [Saad et al. 2012] [Xue *et al.* 2014] [Mittal *et al.* 2012] [Chu *et al.* 2015] [Moorthy *et al.* 2011] [Liu *et al*. 2014] [Moorthy *et al*. 2011] or to particular apps like content created by users, commercial pictures and so on. Nevertheless, not many methods have been developed to assess air quality in actual outdoor settings.

Air pollution prediction using cloud technology involves leveraging cloud-based computing resources and advanced algorithms to analyze environmental data in real-time. This process includes collecting data from various sources such as sensors, satellites, and weather stations, then using machine learning or statistical models to predict air pollution levels. Cloud computing offers scalability, flexibility, and computational power, enabling more accurate and timely predictions. Additionally, cloud-based solutions can facilitate data sharing, collaboration, and accessibility, ultimately supporting better decision-making and management of air quality. We proposed a mist stage assessment technique for outdoor real-world settings in our prior research, which motivated us to use a similar approach to solve the pollutants in the air levels identification issue. The primary metric is still comparing data across the daylight and darkish streams in an individual fuzzy picture. The computing speed is an additional factor. A system with an Intel(R) Core (TM) i7-4790 CPU Corporation Private Limited, Xiamen, running at 3.60 GHz and fitted with twelve gigabytes of Memory takes 2.8 seconds to analyze a snapshot with one million pixels, according to Ref. [Du *et al.* 2024]. For high-resolution or low-power distributed supervisor control systems, this may not be sufficient for real-time processing.

3.2 Property of Insensitive

Utilizing reduced pictures is an obvious approach; consequently, calculation performance can be significantly increased. However, the veracity of the evaluation may be compromised. In previous research [Du *et al.* 2024],we concluded that factors influencing the precision of mist stage evaluations include deviations in the bright canal, modifications to the brightness of both dark and shining transmit priors, precise split of high-contrast as well as low-contrast regions. C^{db} which represents the difference across the bright and darker channels in a given image, is the

most crucial among these variables. In light of this, we employ C db as an illustration for the fresh concept in Figure 4.

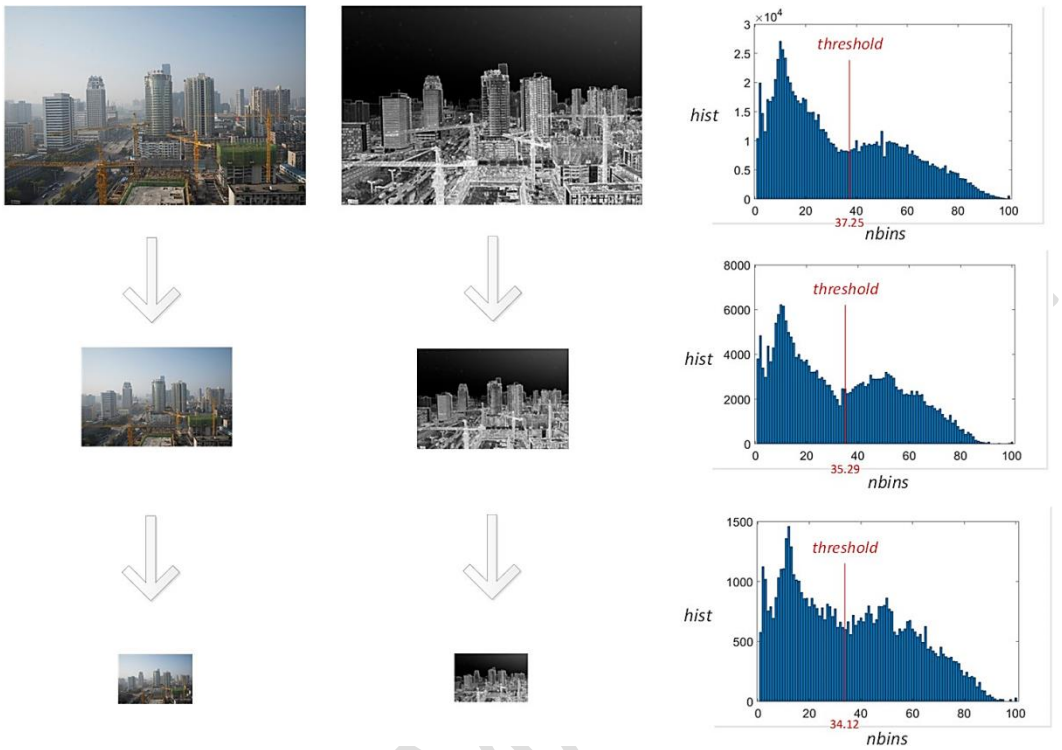

Figure 4. An exemplification of the hypersensitive characteristic of C db. (a) the cropped as well as the original photos. (b) the C db that matches various scales. (c) a segmentation criterion and distribution of the related C dataset

Despite the variations in the dimensions of the indistinct pictures in the first section, the histogram-like morphologies of the associated C db in the last field have extremely comparable, and the splitting criteria are astonishingly comparable as well (Figure 4). Alternatively stated, the division cutoff of the percentile is not impacted by the size of the picture, as the contour of the percentile exhibits self-similarity across scales. Thus, by employing this insensitive attribute as a criterion for evaluating the extent of pollution in the atmosphere, we mitigate our susceptibility to the consequences of picture degradation. Indeed, the human vision system possesses an analogous attribute. The fog of the picture can be viewed alongside quantified by individuals, irrespective of the initial or shortened dimensions.

3. 3 Channel ranging based cloud model

In conclusion, the scale of the input image has no effect on two specific characters. The first is the proportion of dark to light channels preceding the source picture, and the second is a segmentation level for the high-contrast and low-contrast regions. These characteristics are advantageous for air pollution detection endeavors. Downsampling the image to a suitable dimensions allows for the preservation of the initial assessment accurately while significantly

enhancing the pace of the operation. We provide a synopsis of the method's operation below. The just DBCPs statistic by our team is the inspiration for this novel approach, which we refer to as Channel ranging based cloud model [Du *et al.* 2024]. However, Channel ranging based cloud model enables the detection of polluted air levels at a significantly accelerated operation acceleration. Channel ranging based cloud modelcan be defined as follows in Eq (3):

$$\text{Channel ranging based cloud model} \triangleq \frac{1}{w}.\frac{1}{h}.\sum\nolimits_{i=1}^{w}\sum_{j=1}^{h} dbcp(i,j) \tag{3}$$

wherein the derived air pollution level assessment index is denoted by dbcp, and the length and width of each picture are represented by w and h. Estimating the dataset cipher for the image ID is as follows in Eq (4):

$$dbcp(I_D) \triangleq \begin{cases} \frac{C^{db}(I_D)}{t_d(I_D)}, I_D \epsilon \Omega_{\mathrm{h}} \\ T[C^{db}(I_D)], I_D \epsilon \mathrm{I} \end{cases} \tag{4}$$

In the given context, C^{db} denotes the brightness ratio among the darker as well as vibrant channels of the decreased picture ID [He *et al.* 2011] [Wang *et al.* 2013]. The high-contrast as well as low-contrast regions of C^{db} are denoted as Ω_h and Ω_I, as well. td represents the improved spread relate of ID [He *et al.* 2013], and T[•] signifies the worldwide image thresholds of C^{db} as determined by Otsu's approach [Otsu *et al.* 1979]. The definition of the downsampled picture ID is as follows in Eq (5):

$$I_D \triangleq I(\frac{i}{n}, \frac{j}{n}) \tag{5}$$

where (i, j) denotes 2D column as well as row position of every pixel, I(i, j) symbolizes the initial indistinct raw picture, and n signifies the sampling rate number.

3.4 Suggested Method for Protecting Service Provider Information

We simply focus on making sure that the data we transfer to the storage is safe and controlled by a cloud administrator. The recommended method enables a user to safeguard personal data kept in a cloud by the cloud service provider. These days, a person's cell phone is their lifeblood and essential to their personal growth. Yet there are some problems there, such as inadequate processing power, capacity for storage, supply of electricity, and data security. Figure 5 depicts a software functional prototype for the proposed system with the stenography app (SA).

These elements make up our model's core component:

- User: The user's job is to choose a picture and a key-data combination.
- Intelligent mobile gadget capable of executing steganography software
- A programmer for steganography is used to encrypt information along with the key in a picture that the user provides.
- Stego image: These are created by steganography applications and sent to cloud servers. If the user's input key matches, the programmer then pulls information from the picture.

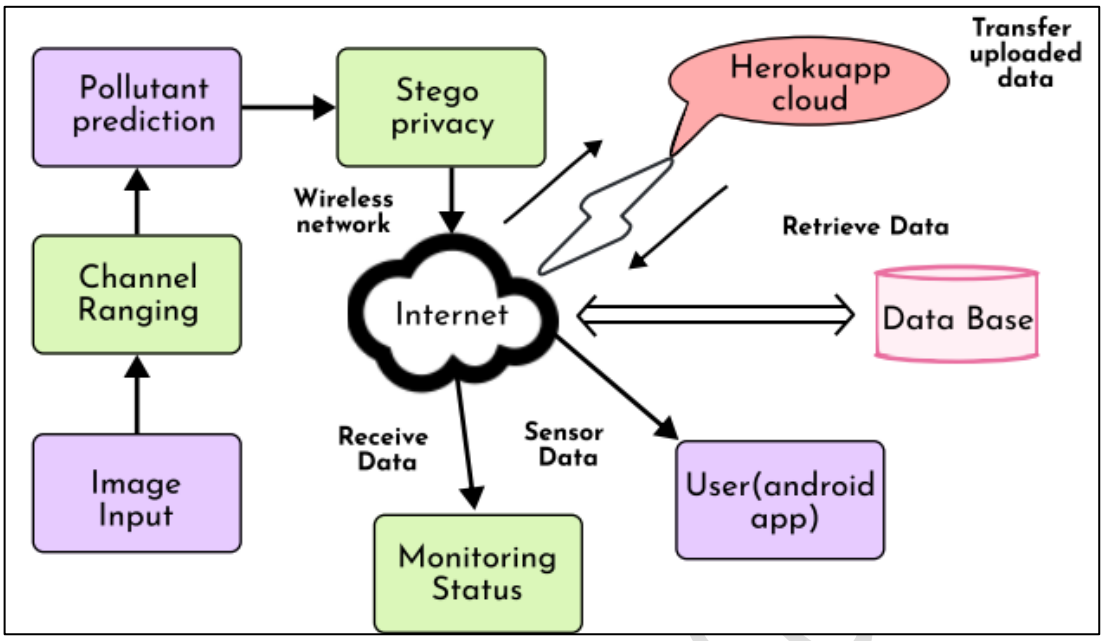

Figure 5: A hybrid of cloud computing and steganography for air pollution monitoring

In this paradigm, the user chooses a picture, then inputs data and keys. The steganography programmed, which has been put in on the user's mobile device, uses this input. The steganography software transforms the inputs and creates steno images that are stored on the cloud. As is well known, using the public cloud needs a link to the internet. If the key matches, the user may securely and conveniently access the cloud-based data. To do this, the user must utilise a steganography programmer. The least important bit strategy, which we utilised in this study to conceal knowledge, making the smartphone cloud computing programme resilient, dynamic, and less susceptible to picture manipulation. Moreover, we'll use 24 bit pictures, which provide 16,000k possibilities that may effectively hide data, making it difficult to distinguish any differences between the altered image and the initial version or real image. Techniques based on encrypting are used to boost security, however doing so will put forth more strain on the CPU and cause it to run slower, which will decrease its speed. We have used the idea of a key to solve this issue. With the use of an algorithm that determines the bytes corresponding to the exact position of the essential the key is now encased into a picture together with actual data or facts. To ensure safe and effective communication, the person using it merely must put in the programmer and remember the key.

4 Experimental Results

The proposed research is analyzed with the RHID_AQI dataset for offering people with a blind standard for assessing the visual quality of fuzzy pictures [Du *et al*. 2024] [Yin *et al.* 2023]. The primary picture collection is from a 2014 Chinese photography exhibit [Ma *et al.* 2018], therefore we developed personal assessment studies on these photos using a single-stimulus

approach. The archive was created using 301 photos that were captured in actual foggy settings within the metropolitan regions of eight contemporary Chinese cities.

In Channel ranging based cloud model, algorithms are two variables that must be experimentally established. The downsampling variable n is the initial one. The applicant must be able to give immediate processing in addition to a strong connection accuracy. We sample the supplied fuzzy pictures to 1/n of the initial dimensions to compute their Channel ranging based cloud model indices in order to evaluate the impact of n. Next, the association coefficient among each of the airborne pollutants indicators—PM2.5, PM10& AQIs and the final goal rating is computed and shown in Figure 6.

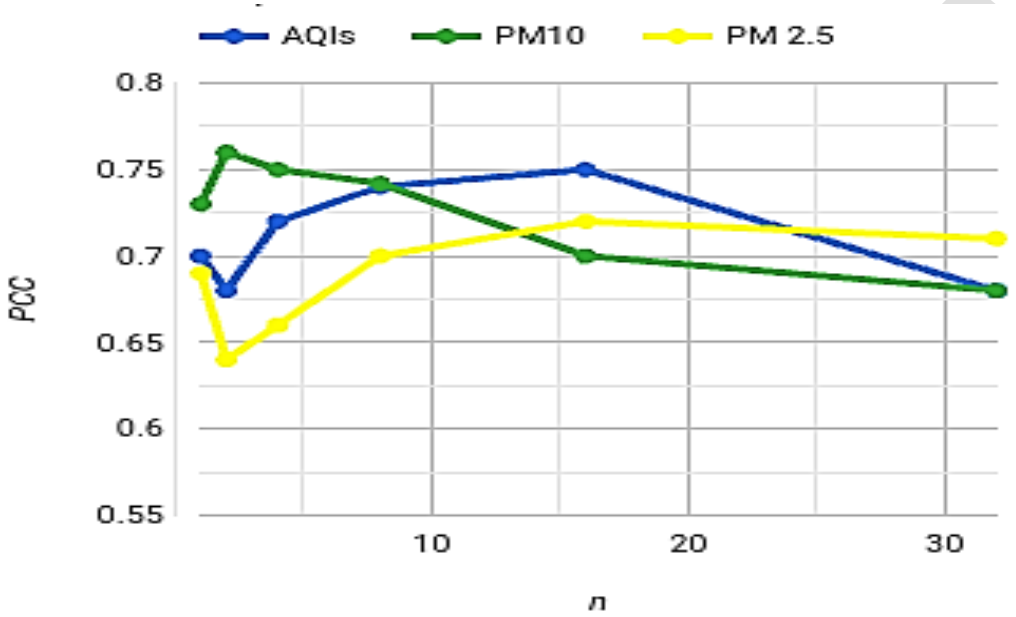

Figure 6: Analyzing how different down sampling parameters affect correlation findings

Figure 6's findings surpass our expectations. It is observed that there is no decline in the association among our visual signal and the air indicators for quality when the picture size is reduced. It surpasses the original dimensions in quality. This phenomenon occurs for all 3 air pollution indices for RHID_AQIs a dataset, including cross-scenes pictures. Figure 6 shows scaling a 1177 × 786 picture down 16 times results in the highest correlation. Therefore, the ideal picture resolutions for a lower picture I***D*** would be within 48 × 48, in which instance the algorithm's outputs would most accurately represent the amount of airborne pollutants. The dimension of the templates windows for the computation of the dark channel preceding and the brilliant channels previous in a single picture is a second factor that has to be established. Following an analysis of the impact of window dimension on haze levels assessments [Du et al. 2024], it was shown that efficiency is insensitive to windows dimension change. The window size should be suitably decreased to correspond with the initial image's scaling when it has been done so; this could reduce the processing time. In Figure 7, we experiment with various frame widths that vary among 3 × 3 to 9 × 9 to see how the parameter affects the data. To achieve the best outcomes, we recommend a window size of 5 × 5.

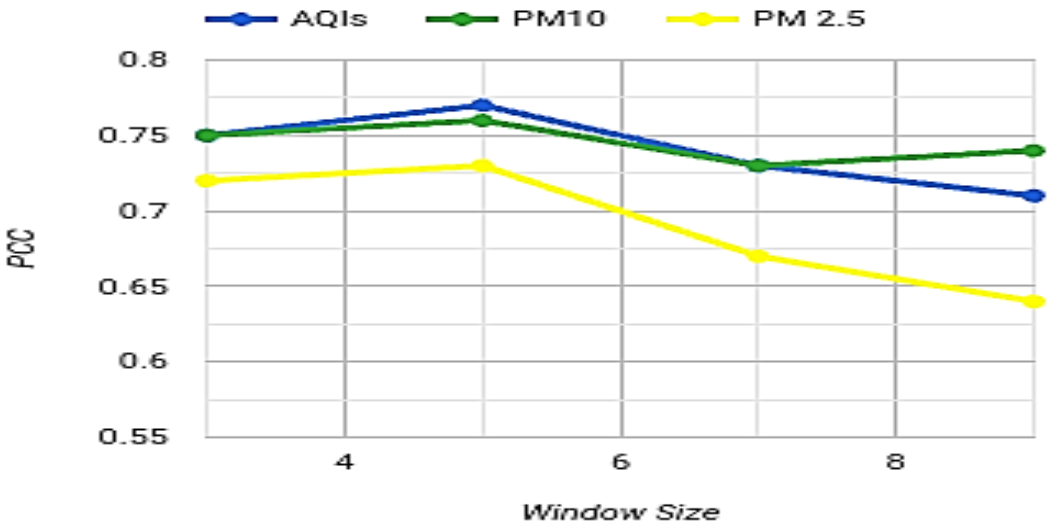

Figure 7:Comparing the relationship data across various window widths

4.1 Comparing the Performance

We calculate the association between the measurements of pollutants in the air and visual indices, respectively, and provide the findings in Table 2 and figure 8. A range of picture qualitative markers based on artificial intelligence or hazy background features, as well as private ratings from the RHID_AQIs datasets, were employed as visual guides to facilitate comparisons. The outcomes meet expectations. In certain cases, the measurable metrics may even do better than the emotional MOS score. The deep learning approach DIQaM-NRs and our measurement hold the lead across these both. But as we shall see in the next part, the suggested Channel ranging based cloud model method is faster overall, making it a superior approach in general.

Table 2.Using the RHID_AQIs information set, PCC is compared among visual indices and AQIs

Techniques	AQIs	PM2.5	PM10
MOSs	0.72	0.72	0.71
R	0.69	0.67	0.72
T	0.33	0.37	0.31
C	0.69	0.67	0.75
μ	0.35	0.37	0.31
Mean	0.20	0.10	0.32

Variance	0.54	0.49	0.61
E	0.65	0.64	0.68
D	0.76	0.68	0.73
DBCPs-I	0.69	0.70	0.74
DBCPs-II	0.70	0.76	0.76
DBCPs-III	0.72	0.78	0.73
CNNs	0.69	0.68	0.76
DIQaMs-NRs	0.76	0.77	0.77
Channel ranging based cloud model	0.76	0.76	0.75

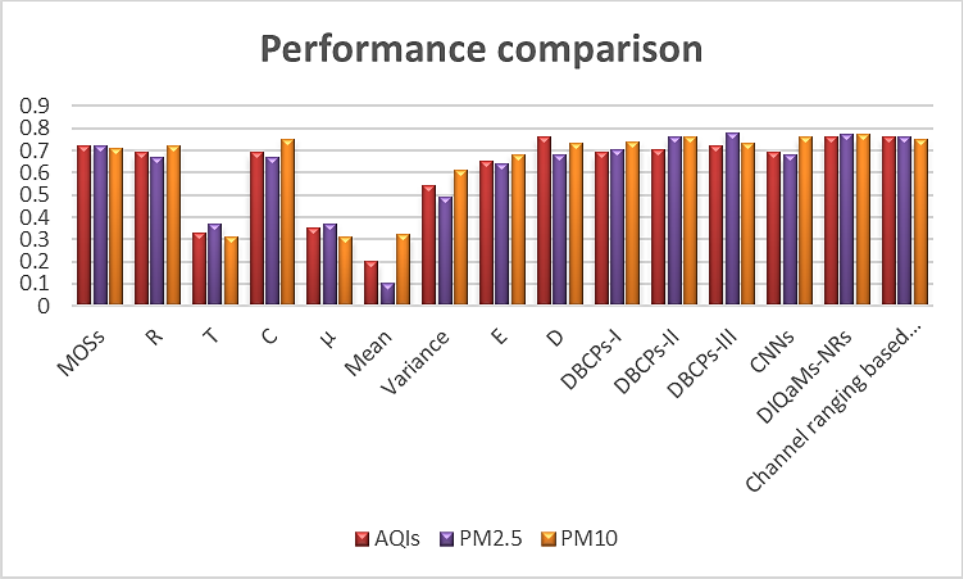

Figure 8: Performance comparison against Channel ranging based cloud model

4.2 Costing Computation

Figure 9 shows the median time required to compute for each picture, which helps us evaluate the computational price even further. The operation time reduces exponentially, as the graphic illustrates. As an illustration, for n = 1 and n = 16, every image's processing time is lowered from 2.58 s to 0.08 s, resulting in a 32-fold improvement in efficiency of computation. A real-time surveillance system for the atmosphere will benefit from this speed increase. Figure 9 shows similar computation speeds around n = 16. In light of this, it is recommended to ensure the downsampled picture resolution (Un) not fall below 48 × 48 in dimensions, with regard to both effectiveness and speed.

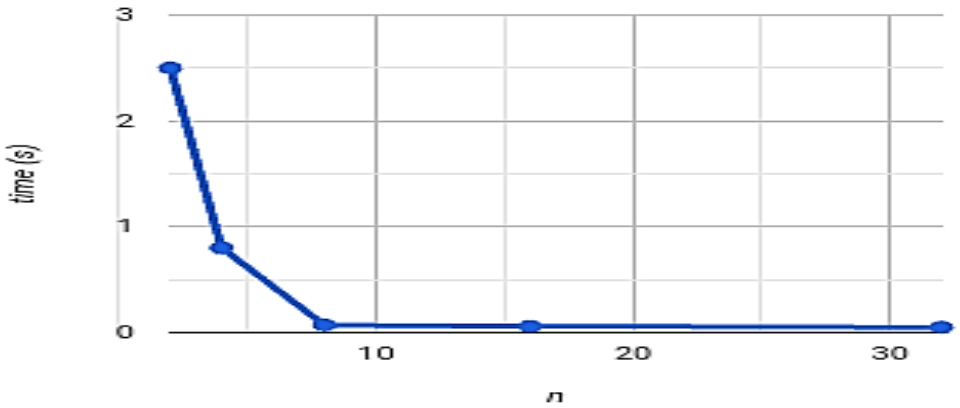

Figure 9: Evaluation of computing costs using the down-sampling approach

We choose comparatively excellent candidates to contrast their computational abilities using Table 2's subjective measures' effectiveness. Our CPU PC is configured with an Intel(R) Core (TM) i7-4790 CPU running at 3.60 GHz &twelve gigabytes of Memory. Table 3 displays the mean time spent computing each picture. Clearly, Channel ranging based cloud model outperforms the nearby deep learning technique by a factor of 10 when it comes to efficiency.

Table 3: Analysis of calculation costs for various measures used in the RHID_AQI dataset to assess picture quality.

Techniques	R	C	ENTROPY	D	DBCPs-I	DBCPs-II	DBCPs-III	CNNs	DIQaMs-NRs	Channel ranging based cloud model
Time (sec)	1.35	0.08	0.03	1.87	2.80	1.55	2.81	0.34	0.82	0.09

4.4 Utilisation in Surveillance Systems in Real-Time

The use of the suggested approach in the area of air pollution measurement is mostly described in the preceding section. In fact, the Channel ranging based cloud model technique has an opportunity to be used in a variety of real-time tracking. For instance, in a self-driving situation [Johari *et al.* 2020], it is capable of tracking the air condition of the road surface. Quick alerts may be sent when foggy conditions pose a significant risk to driver safety.

Furthermore, the Channel ranging based cloud modelscore shows a substantial link with picture visual quality, which reflects the degree of haziness in real-world surroundings, as demonstrated in Table 4. Nevertheless, it offers a tenfold or higher benefit when it comes of computation speed. One important property that makes it possible to utilise it in continuous surveillance systems is its swift processing capability. As seen in Figure 10, it may be used as an additional visual measure to identify other disastrous climatic conditions, including wildfires [Ichoku *et al.* 2005], tornadoes [Jun *et al.* 2019], and so forth, that share visual features with

foggy weather. Channel ranging based cloud modelBenefits in various application situations will be its quickness.

Table 4:Comparing PCC across several quality of images indices and subjective ratings using the RHID_AQIs dataset

Techniques	R	C	ENTROPY	D	DBCPs-I	DBCPs-II	DBCPs-III	CNNs	DIQaM-NRs	Channel ranging based cloud model
PCCs	0.80	0.82	0.71	0.85	0.89	0.95	0.96	0.86	0.94	0.97

(a) **(b)** **(c)**

Figure 10. Images of ordinary polluted weather include: (a) a dense fog [38], (b) haze from wildfires [Mukundan *et al.* 2022], and (c) a tornado [Shau *et al*. 2022]

5 Conclusions

In this study, we delve into the intriguing question of how humans perceive air quality, particularly pollution levels, through imagery analysis. Through rigorous study and validation, we have arrived at several significant findings. The Channel ranging based cloud model, not only outperforms previous methods in terms of speed but also exhibits a stronger correlation with air quality indices. This makes it a highly promising candidate for integration into specialized air pollution monitoring networks. Lastly, the innovative measure we propose holds potential for practical implementation in real-time air pollution warning systems. By alerting to deteriorating air quality conditions, it could serve as a valuable tool for enhancing public health and safety. Additionally, its application extends to other domains such as hazy weather surveillance for autonomous driving, tornado monitoring for weather prediction, and wildfire forecasting for disaster preparedness. Response: Proposed algorithm with O(log n) complexity is highly efficient, as the time taken for execution grows slowly even with a large input size. This makes them suitable for handling large datasets or performing complex computations with minimal overhead.But there is still more to be done to further our present research. For instance, the lack of other datasets that are freely accessible including objective picture assessments and air quality markers prevents Channel ranging based cloud model from being compared and verified against different datasets. Furthermore, we want to use our indicators for use in a video monitoring system; however, as of right now, no air quality indicator data are available, while there are only a few outdoors picture and image quality assessment datasets for foggy weather. In

order to test the efficiency of Channel ranging based cloud modelon those data sets and demonstrate or validate the underlying link and process of indoor air quality and seeing, future studies ought to determine and construct outside photographs or videos data that give more reliable air indicators for quality.

References

[1] Preethi P., Saravanan T., Mohanraj R. and Gayathri P.G. (2024), A real-time environmental air pollution predictor model using dense deep learning approach in IoT infrastructure, 26(3), 05666.

[2] Sallis P., Dannheim C., Icking C. and Maeder M. (2014), Air pollution and fog detection through vehicular sensors, In Proceedings of the 8th Asia Modelling Symposium, Taipei, Taiwan, 23–25 September, pp. 181–186.

[3] Mukundan A., Huang C., Men T.C., Lin F.C. and Wang H.C. (2022), Air pollution detection using a novel snap-shot hyperspectral imaging technique, Sensors 22, 6231.

[4] Wen Z., Wang Q., Ma Y., Jacinthe P. A., Liu G., Li S. and Song K. (2024), Remote estimates of suspended particulate matter in global lakes using machine learning models, InternationalSoilandWaterConservationResearch,12(1),200216,doi:https://doi.org/10.1016/j.iswcr.2023.07.002.

[5] Min X., Zhai G., Gu K., Yang X. and Guan X. (2019), Objective quality evaluation of dehazed images, IEEE Trans, Intell, Transp, Syst, 20, 2879–2892.

[6] Li B., Ren W., Fu D., Tao D., Feng D., Zeng W. and Wang Z. (2019), Benchmarking single-image dehazing and beyond, IEEE Trans, Image Process, 28, 492–505.

[7] Wen Z., Shang Y., Lyu L., Tao H., Liu G., Fang C. and Song K. (2024), Re-estimating China's lake CO2 flux considering spatiotemporal variability, Environmental Science and Ecotechnology, 19, 100337, doi: https://doi.org/10.1016/j.ese.2023.100337.

[8] Zhao S., Zhang L., Huang S., Shen Y. and Zhao S. (2020), Dehazing evaluation: Real-world benchmark datasets, criteria, and baselines, IEEE Trans, Image Process, 2020, 29, 6947–6962.

[9] Jiang H., Wang M., Zhao P., Xiao Z., and Dustdar S. (2021), A Utility-Aware General Framework With Quantifiable Privacy Preservation for Destination Prediction in LBSs,IEEE/ACM Trans, Netw, 29(5), 2228-2241, doi: 10.1109/TNET.2021.3084251.

[10] Korhonen J. (2019), Two-level approach for no-reference consumer video quality assessment, IEEE Trans, Image Process, 28, 5923–5938.

[11] Du W. and Wang G. (2013), Intra-Event Spatial Correlations for Cumulative Absolute Velocity, Arias Intensity, and Spectral Accelerations Based on Regional Site Conditions. Bulletin of the Seismological Society of America, 103(2A), 1117-1129, doi: 10.1785/0120120185.

[12] Fu X., Lin Q., Guo W., Ding X. and Huang Y. (2013), Single image dehaze under non-uniform illumination using bright channel prior, J, Theor, Appl, Inf, Technol, 48, 1843–1848.

[13] Kang L., Ye P., Li Y. and Doermann D. (2014), Convolutional neural networks for no-reference image quality assessment, In Proceedings of the 2014 IEEE Conference on Computer Vision and Pattern Recognition, Columbus, OH, USA, 23–28 June , pp. 1733–1740.

[14] Zhang S., Bai X., Zhao C., Tan Q., Luo G., Wang J. and Xi H. (2021), Global CO2 Consumption by Silicate Rock Chemical Weathering: Its Past and Future, Earth's Future, 9(5), e1938E-e2020E, doi: https://doi.org/10.1029/2020EF001938.

[15] Bosse S., Maniry D., Müller K.R., Wiegand T. and Samek W. (2018), Deep neural networks for no-reference and full-reference image quality assessment, IEEE Trans, Image Process, 2018, 27, 206–219.

[16] Du C., Bai X., Li Y., Tan Q., Zhao C., Luo G. and Yang S. (2024), Storage, form, and influencing factors of karst inorganic carbon in a carbonate area in China, Science China Earth Sciences, doi: 10.1007/s11430-023-1249-9.

[17] Yin Z., Liu Z., Liu X., Zheng W. and Yin L. (2023), Urban heat islands and their effects on thermal comfort in the US: New York and New Jersey, Ecological Indicators, 154, 110765. doi: https://doi.org/10.1016/j.ecolind.2023.110765.

[18] Ma K., Liu W., Zhang K., Duanmu Z., Wang Z. and Zuo W. (2018), End-to-end blind image quality assessment using deep neural networks, IEEE Trans, Image Process, 27, 1202–1213.

[19] Shang K., Xu L., Liu X., Yin Z., Liu Z., Li X. and Zheng W. (2023), Study of Urban Heat Island Effect in Hangzhou Metropolitan Area Based on SW-TES Algorithm and Image Dichotomous Model, SAGE Open, 13(4). doi: https://doi.org/10.1177/21582440231208851.

[20] Ancuti C.O., Ancuti C. and Timofte R. (2020), NH-HAZE: An image dehazing benchmark with non-homogeneous hazy and haze-free images, In Proceedings of the IEEE Computer Society Conference on Computer Vision and Pattern Recognition Workshops, Seattle, WA, USA, pp. 1798–1805.

[21] Kamani H., Baniasadi M., Abdipour H., Mohammadi L., Rayegannakhost S., Moein H., and Azari A. (2023), Health risk assessment of BTEX compounds (benzene, toluene, ethylbenzene

and xylene) in different indoor air using Monte Carlo simulation in zahedan city, Iran. Heliyon, 9(9).

[22] Oliveira M., Slezakova K., Delerue-Matos C., Pereira M.C. and Morais S. (2019), Children environmental exposure to particulate matter and polycyclic aromatic hydrocarbons and biomonitoring in school environments: A review on indoor and outdoor exposure levels, major sources and health impacts. Environ. Int. 2019, 124, 180–204.

[23] Wang Z., Bovik A.C., Sheikh H.R. and Simoncelli E.P. (2004), Image quality assessment: From error visibility to structural similarity, IEEE Trans, Image Process, 2004, 13, 600–612.

[24] Saad M.A., Bovik A.C. and Charrier C. (2012), Blind image quality assessment: A natural scene statistics approach in the DCT domain. IEEE Trans, Image Process, 21, 3339–3352.

[25] Xue W., Mou X., Zhang L., Bovik A.C. and Feng X. (2014), Blind image quality assessment using joint statistics of gradient magnitude and Laplacian features, IEEE Trans, Image Process, 23, 4850–4862.

[26] Mittal A., Moorthy A.K. and Bovik A.C. (2012), No-reference image quality assessment in the spatial domain, IEEE Trans, Image Process, 2012, 21, 4695–4708.

[27] Chu Y., Mou X., Fu H. and Ji Z. (2015), Blind image quality assessment using statistical independence in the divisive normalization transform domain, J, Electron, Imaging, 24, 063008.

[28] Moorthy A.K. and Bovik A.C. (2010), A two-step framework for constructing blind image qualityindices, IEEE Signal Process, Lett, 17, 513–516.

[29] Liu L., Dong H., Huang H. and Bovik A.C.(2014), No-reference image quality assessment in curvelet domain, Signal Process, Image Commun, 29, 494–505.

[30] Moorthy A.K. and Bovik A.C. (2011), Blind image quality assessment: From natural scene statistics to perceptual quality, IEEE Trans, Image Process,20, 3350–3364.

[31] He K., Sun J. and Tang X. (2011), Single image haze removal using dark channel prior. IEEE Trans. Pattern Anal, Mach, Intell, 33, 2341–2353.

[32] Wang Y.T., Zhuo S.J., Tao D.P., Bu J.J. and Li N. (2013), Automatic local exposure correction using bright channel prior for under-exposed images, Signal Process, 93, 3227–3238.

[33] He K., Sun J. and Tang X. (2013), Guided image filtering, IEEE Trans, Pattern Anal, Mach, Intell, 35, 1397–1409.

[34] Otsu N. (1979), A threshold selection method from gray-level histograms, IEEE Trans, Syst, Man Cybern, 9, 62–66.

[35] Johari A. and Swami P.D. (2020), Comparison of autonomy and study of deep learning tools for object detection in autonomous self driving vehicles, In Proceedings of the 2nd International Conference on Data, Engineering and Applications, Bhopal, India, 28–29; pp. 1–6.

[36] Ichoku C. and Kaufman Y.J. (2005), A method to derive smoke emission rates from MODIS fire radiative energy measurements, IEEE Trans, Geosci, Remote Sens, 43, 2636–2649.

[37] Jun L., Honggen Z., Jianbing L. and Xinan L. (2019), Research on the networking strategy of tornado observation network in northern Jiangsu based on X-band weather radar, In Proceedings of the 2019 International Conference on Meteorology Observations, Chengdu, China, 28–31; pp. 1–4.

[38] Smog in Beijing. (2013), Available online: http://www.cd-pa.com/bbs/thread-572953-1-1.html.

[39] Mukundan A., Huang C.C., Men T.C., Lin F.C. and Wang H.C. (2022), Air pollution detection using a novel snap-shot hyperspectral imaging technique, Sensors 22, 6231.

[40] Sahu G., Seal A., Bhattacharjee D., Nasipuri M., Brida P. and Krejcar O. (2022), Trends and prospects of techniques for haze removal from degraded images: A survey, IEEE Trans, Emerg, Top, Comput, Intell, 2022, 6, 762–782.